BIOCHEMISTRY
including biophysical chemistry & molecular biology

Article

pubs.acs.org/biochemistry

Ca^{2+} Interacts with Glu-22 of Aβ(1−42) and Phospholipid Bilayers to Accelerate the Aβ(1−42) Aggregation Below the Critical Micelle Concentration

Xinyao Yi,[†,‡] Yi Zhang,[‡] Ming Gong,[†] Xiang Yu,[§] Narek Darabedian,[†] Jie Zheng,[*,§] and Feimeng Zhou[*,†]

[†]Department of Chemistry and Biochemistry, California State University, Los Angeles, California 90032, United States
[‡]College of Chemistry and Chemical Engineering, Central South University, Changsha, Hunan 410083, P. R. China
[§]Department of Chemical and Biomolecular Engineering, The University of Akron, Akron, Ohio 44325, United States

ABSTRACT: The amyloid cascade hypothesis links the amyloid-β (Aβ) peptide aggregation to neuronal cell damage and ultimately the etiology of Alzheimer's disease (AD). Although Aβ aggregation has been known to accelerate at cell membranes, the exact mechanism of Aβ peptide deposition and the involvement of extracellular species are still largely unclear. Using surface plasmon resonance (SPR) and atomic force microscopy (AFM), we demonstrate that Ca^{2+} ions, in conjunction with lipid bilayer, lower the threshold concentration for Aβ aggregation (>a few micromolar in vitro) to physiological levels (low nanomolar). Circular dichroism spectroscopy reveals that Ca^{2+} ions and the lipid bilayer concertedly accelerate the conformational change or misfolding of Aβ peptides. Molecular dynamics calculation indicates that Ca^{2+} is sandwiched between Glu-22 of Aβ and the lipid phosphate group. SPR experiments conducted using an E22G mutant confirmed the strong interaction among Ca^{2+}, Aβ(1−42), and the phospholipid bilayer. With the C- and N-termini of the Aβ dimer fully exposed for the attachment of additional Aβ molecules, fibrils formed with the Ca^{2+}-anchored Aβ nuclei appear to interact with lipid bilayers differently from those preformed in solution. Thus, similar to the role of Ca^{2+} in enriching islet amyloid polypeptides in the pancreas of diabetic patients (*Biophys. J.* 2013, *104*, 173−184) and the "Ca^{2+} bridge" in mediating membrane interaction with α-synuclein in the Parkinson's disease (*Biochemistry*, 2006, *45*, 10947−10956), the influence of Ca^{2+} on the Aβ adsorption at cell membranes, which leads to neuronal membrane damage in AD, cannot be overlooked.

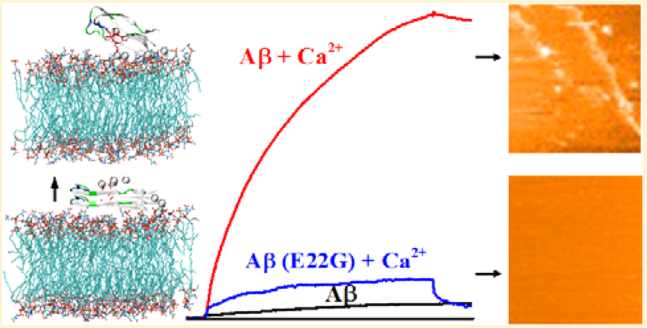

A number of major neurodegenerative diseases, such as Alzheimer's disease (AD), Parkinson's disease (PD), and type-2 diabetes, are linked to the accumulation of aggregates of misfolded peptides or proteins. The amyloid cascade hypothesis presumes that AD is caused by damages associated with aggregation of amyloid-β peptides (Aβ) comprising 39−43 amino acid residues.[1−3] In solution, monomeric amyloid proteins/peptides are unstructured but can convert and assemble into small nuclei containing different amounts of β-structures. These nuclei further stack up in a highly ordered fashion to elongate into fibrils[4] via a nucleation−polymerization mechanism.[5−8] Thus, a minimal concentration of Aβ monomers is required for the formation of the oligomer-containing nuclei.[9,10] In vitro Aβ nucleation only occurs above its critical micelle concentration (CMC), which is in the range of 6−100 μM.[11−13] The CMC value is orders of magnitude higher than Aβ found in physiological milieu. For example, in cerebrospinal fluids (CSFs), Aβ is present only between 0.6 and 10 nM.[14−18] A question that has been investigated intensely[19−21] is why a vast difference exists between the in vitro and in vivo Aβ concentrations for aggregation, even though fibrils produced in both scenarios are comparable in their morphologies.[15]

One of the rationales is that the cell membrane can help lower the threshold value for in vitro nucleation and fibrillation by serving as a two-dimensional template for the formation Aβ seeds or nuclei.[22−24] Membrane has been shown to possess physical properties that facilitate the adsorption of peptides/proteins without significantly affecting their translational mobility[9,25,26] as well as the electrostatic interaction between the lipids and Aβ.[27,28] As a result, additional molecules can be accumulated through interpeptide interaction along the membrane surface, eventually forming nuclei that are critical for fibril formation. Various lipid membranes have been shown to enrich Aβ peptides, facilitating misfolding of Aβ into toxic oligomers at rates considerably faster than in a membrane-free environment.[27,29,30] Using single molecule spectroscopy, two independent studies have shown that at 100−150 nM Aβ(1−40) adsorbs onto supported phospholipids[19] and PC12 cells within a few hours or at 2 nM Aβ(1−40) produces oligomers at cell membranes after 6 days.[21] Regarding the modes of

Received: June 26, 2015
Revised: September 21, 2015
Published: October 1, 2015

DOI: 10.1021/acs.biochem.5b00719
Biochemistry 2015, 54, 6323−6332

interaction between Aβ and lipid bilayer/membrane surfaces, different and conflicting models have been proposed. Some suggest that monomeric Aβ peptides are attached parallel to the bilayer surface in an α-helical conformation.[31] Others have posited that monomers can insert into the membrane as α-helices and eventually reemerge to the lipid surface as β-sheet-structures. In addition, it has been suggested that Aβ oligomers interact with lipid membranes by forming transmembrane pores or inducing membrane thinning and curvature, both of which could induce abnormal ion homeostasis and oxidative damages in membranes.[9,25,32,33]

Despite the intensive effort to elucidate the relationship between Aβ adsorption/aggregation and membrane constituents/structures, the effect of extracellular species on the accumulation of Aβ at membranes or lipid bilayers has not been investigated in detail. For example, Bokvist and Gröbner showed that misfolding of amyloidogenic proteins is influenced by polymers added into solution that mimic the crowded cellular milieu.[29] The study on the role of calcium ions in amyloid diseases has been concerned with how amyloid proteins and their interactions with membrane disrupt Ca^{2+} conductivity and signaling (i.e., the calcium hypothesis).[34−36] Several neurotrophic factors that alleviate the adverse effect of Aβ aggregation have also been found to stabilize the intracellular calcium level.[35] On the other hand, changes in cytosolic calcium concentrations could up-regulate the amyloid precursor protein (APP) and hence the production of Aβ peptides. It is still under debate whether calcium dyshomeostasis is the cause[37] or the result[38,39] of Aβ aggregation and/or the accompanying changes in cell membranes. To our surprise, the effect of Ca^{2+} on the initial Aβ adsorption and subsequent aggregation at cell membranes, lipid bilayers, or liposomes has not been investigated experimentally, even though such an effect has been documented for other amyloidogenic proteins/peptides.[40,41] For example, the enrichment of islet amyloid polypeptide (IAPP), a chief constituent of amyloid deposits in the pancreatic islets of diabetic patients, was found to enrich at the membrane surface and subsequently self-assemble into oligomers in the presence of Ca^{2+}.[40,42] Ca^{2+} bridges have been shown to mediate the interaction between the membrane and the acidic tail of α-synuclein, a protein implicated in the neuropathology of Parkinson's disease.[41] The effect was likened to the Ca^{2+}-induced conformational change in calcium/phospholipid binding proteins such as annexin.[41]

In our previous molecular dynamics calculation about the effect of cholesterol on the Aβ interaction with lipids, calcium ions were consistently found to interact with unstructured Aβ monomers, and the resultant Aβ−Ca^{2+} complex interacts with the phosphate headgroups of 1-palmitoyl-2-oleoylphosphotidylcholine (POPC).[43] However, the interaction among Ca^{2+}, Aβ, and lipid was not verified experimentally, and the negatively charged amino acid residue(s) that interact with Ca^{2+} was (were) not pinpointed. In addition, it is not clear whether Ca^{2+} will accelerate the adsorption of Aβ at a concentration substantially lower than the CMC. We envision that results from such an investigation should help shed light on the aforementioned difference in the nucleation concentration threshold between in vitro and in vivo Aβ aggregations.

Here we report on our computational and experimental studies about the roles of Ca^{2+} and Glu-22 in Aβ(1−42) accumulation at the solution/lipid bilayer interface. Our data indicate that aggregates of Aβ(1−42) can be formed at an Aβ(1−42) concentration that is 2 orders of magnitude (~50 nM) lower than the Aβ(1−42) CMC. MD simulations also indicate the interaction among Ca^{2+}, Glu-22 of Aβ, and phosphate on the lipid headgroup. Our results strongly suggest that the orientation of Aβ(1−42) in the presence of Ca^{2+} is favorable for the accumulation of additional Aβ(1−42) molecules from solution. The Aβ(1−42) oligomers and fibrils formed with Ca^{2+}-anchored nuclei to lipid bilayers interact with the lipid bilayers differently than those preformed in solution. Possible linkage between the calcium and amyloid hypotheses is discussed.

MATERIALS AND METHODS

Chemicals and Materials. Triethylene glycol mono-11-mercaptoundecyl ether ($HSC_{11}PEG_3$-OH), NaH_2PO_4, and Na_2HPO_4 were acquired from Sigma (St. Louis, MO). $CaCl_2$, NaCl, methanol, and chloroform were purchased from Fisher Scientific (Pittsburgh, PA). Aβ(1−42) and Aβ(1−28) peptides were available from American Peptide Inc. (Sunnyvale, CA). Aβ(1−28)(E22G) was synthesized in house on a Biotage Sp Wave peptide synthesizer (Uppsala, Sweden). Lipids used in this work, 1,2-dipalmitoyl-*sn*-glycero-3-phospho-L-serine sodium salt (DPPS), 1-palmitoyl-2-oleoyl-*sn*-glycero-3-phospho-(1′-*rac*-glycerol) sodium salt (POPG), and 1,2-dipalmitoyl-*sn*-glycero-3-phosphocholine (DPPC) were purchased from Avanti Inc. (Alabaster, AL). All aqueous solutions were prepared daily with deionized water. Monoclonal antibodies specific to the N-terminus (clone 6E10) and C-terminus (clone 12F4) of Aβ(1−42) were obtained from Covance Inc. (Dedham, MA).

Solution Preparation. Monomeric and preaggregated Aβ peptides were diluted with phosphate-buffered saline (PBS; 10 mM each for Na_2HPO_4, NaH_2PO_4, and NaCl, pH = 7.4). The artificial CSF (aCSF) contains 150 mM NaCl, 3 mM KCl, 1.4 mM $CaCl_2$, and 0.8 mM $MgCl_2$ in phosphate buffer (10 mM).

Aβ(1−42) Pretreatment. The commercial Aβ sample was first kept in 1,1,1,3,3,3-hexafluoro-2-propanol (HFIP) for 2 h. After a 30 min sonication, the solution was centrifuged at 14 000 rpm for 30 min to remove any insoluble particles. The supernatant was taken out for freeze-drying, which removed HFIP, and the lyophilized Aβ(1−42) was dissolved in NaOH as a 0.25 mM stock solution for further sample preparation. The preaggregated Aβ(1−42) were formed by incubating Aβ(1−42) monomer solution at 37 °C for a predetermined period of time.

Supported Lipid Bilayers. Supported phospholipid bilayers were prepared on mica by casting a droplet of vesicle solution used for the AFM studies. The vesicle solution was formed via a modified fusion method.[44] DPPS, DPPC, POPG, or the DPPS/DPPC mixture (1:1) was dissolved in a mixture of chloroform and methanol (V/V = 9/1) and subsequently dried under N_2. The resultant DPPS pellets were vacuum-desiccated for 1 h to remove residual solvents. The lipid film was resuspended in PBS to a concentration of 1 mg/mL and sonicated for 30 min until a clear solution was obtained. This was followed by seven freeze−thaw cycles. To produce the supported lipid bilayers on SPR chips, $HSC_{11}PEG_3$-OH dissolved in anhydrous ethanol was first coated onto the SPR sensor chips. The vesicle solution was then cast onto the polyethylene glycol self-assembled monolayer[45] at a tempreture higher than the transition tempreture. After incubation at 4 °C overnight, excess solution was washed off with PBS.[44] To study the effect of Ca^{2+}, a drop of 10 mM $CaCl_2$ was cast onto the preformed lipid bilayers for 30 min. The surface was then rinsed with phosphate buffer and dried with N_2.

DOI: 10.1021/acs.biochem.5b00719
Biochemistry 2015, 54, 6323−6332

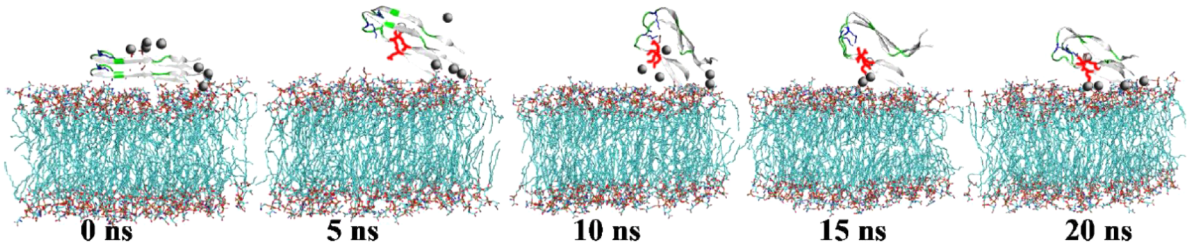

Figure 1. MD snapshots of an Aβ(17−42) dimer on a DPPS bilayer at simulation times of 0, 5, 10, 15, and 20 ns. The hydrophobic residues of the dimer are depicted in gray, hydrophilic residues in green, positively charged residues in blue, and negatively charged residues in red. Calcium ions are shown as gray spheres.

Surface Plasmon Resonance (SPR). The SPR measurements were conducted on a BI-SPR 4000 system (Biosensing Instrument Inc., Tempe, AZ). Running buffer was degassed under a vacuum for 30 min. Samples were preloaded into a 200-μL sample loop and then injected to the flow cell by a syringe pump (model KDS260, KD Scientific, Holliston, MA) at a flow rate of 10 μL/min.

Circular Dichroism (CD) Spectroscopy. CD spectra were collected on a J-810 spectropolarimeter (Jasco Inc., Tokyo, Japan) at room temperature in a cuvette with a 0.1 cm path. The spectra were recorded at a 0.5 nm interval from 260 to 190 nm. Each spectrum is the average of six scans.

Atomic Force Microscopy (AFM). In situ AFM images were obtained on an MFP 3D AFM system (Asylum Research, Santa Barbara, CA). The close-loop scanner allows large surface areas to be imaged without distortion. The scanning speed was typically 0.5 Hz.

Aβ Model. Aβ monomer was derived from NMR data of Aβ(17−42) protofibril structure (PDB code 2BEG).[46] The Aβ(17−42) monomer consists of two β-strands, β1 (residues V17−S26) and β2 (residues I31−A42), connected by a U-bent turn spanning four residues (N27−A30).[46,47] Residues 1−16 at the N-terminus were excluded from the simulation because of their disordered and unsolved structure. Inclusion of an arbitrarily defined Aβ(1−16) structure will lead to ambiguous or even erroneous results. A number of in vitro and in vivo studies have shown that Aβ(17−42) (known as p3), Aβ(9−42) (referred to as N7), and full-length Aβ(1−42) exhibited similar amyloidogenic properties in terms of their aggregation behavior, aggregate morphology, and aggregate-elicited cell toxicity.[48−50] An Aβ(17−42) dimer was constructed by packing Aβ(17−42) monomers on top of each other in a parallel and registered manner, with an initial peptide−peptide separation distance of ∼4.7 Å, according to the experimental data.[46] The N- and C-termini of Aβ(17−42) were capped with charged $-NH_3^+$ and $-COO^-$ groups, respectively.

Molecular Docking. First, an Aβ dimer was docked to the DPPS bilayer by using the PatchDock[51] simulation method that only allows the interface residues to be flexible. The lipid bilayer contained 148 DPPS chains (74 DPPS each side), spanning an area of 68.28 Å × 68.28 Å. The top 100 Aβ-DPPS pairs within the clustering root-mean-square deviation (RMSD) of 4 Å were then subject to the FireDock[52] simulation to optimize the Aβ-DPPS interaction by allowing both rigid-body adjustment and flexible backbone/side chain movements between Aβ and DPPS. The top five Aβ-DPPS pairs from the FireDock simulations are similar in position and orientation to the Aβ dimer on the DPPS. Specifically, both β-strands of the β-hairpin are in contact with the DPPS bilayers.

MD Simulation. The initial DPPS bilayer was constructed using the CHARMM-GUI membrane builder (www.charmm-gui.org),[53] as reported in our previous works.[43,54] The DPPS bilayer, consisting of 119 lipids in each top and bottom leaflet (i.e., total 2 × 119 = 238 lipids), has a size of ∼90 Å × 90 Å in the x−y plane, which is large enough to accommodate the Aβ dimer with a minimal distance of 15 Å between any edge of DPPS bilayer and Aβ. The Aβ-DPPS system used for the docking simulation was solvated in a TIP3P water box. Ca^{2+} and Cl^- ions were also added to achieve an electrically neural system with an ionic strength of ∼100 mM. The resulting system was subject to 5000 steps of the steepest descent minimization with position constraints on heavy atoms of Aβ peptides. This was followed by additional 5000 steps of conjugate gradient minimization without any position constraint. After energy minimization, a series of dynamic cycles were performed to equilibrate the systems from a pre-equilibrium stage to a production-run stage. In the pre-equilibrium stage, the systems were gradually heated from 0 to 300 K with the harmonic position restraints on peptides and lipids being gradually removed every 100 ps to optimize peptide−lipid and peptide−water interactions. The entire pre-equilibrium runs were 1 ns to generate the starting configurations for the production runs. In the production stage, all simulations were performed for 20 ns under the NPAT (constant number of atoms, pressure = 1 atm, surface area, and temperature = 300 K) ensemble. Short-range van der Waals (VDW) interactions were calculated by a switch function with a twin cutoff at 10 and 12 Å, while long-range electrostatic interactions were calculated by a force shift function with a cutoff at 14 Å. All hydrogen atoms were constrained using RATTLE so that a time step of 2 fs was used in velocity verlet integration. The system consisted of an Aβ dimer, a DPPS bilayer, explicit water molecules, and counterions, up to a total of ∼11 000 atoms. Each system was run twice for validation with the same starting coordinates but different initial random velocities. MD trajectories were saved every 2 ps for analysis.

RESULTS

Figure 1 depicts a series of MD snapshots of an Aβ dimer on DPPS bilayer at different simulation times. The choice of a dimer is based on the fact that Aβ(1−42) dimerizes rapidly in solution, and thus dimers could serve as the smallest nucleation seeds for amyloid propogation.[55−57] Moreover, dimerization and oligomerization were found to further accelerate with an increase in β-sheets in the presence of lipid bilayers (vide infra). It is interesting to note that within the first 5 ns, the Aβ dimer reorients by gradually moving its C-terminus away from the lipid bilayer while tilting the N-terminal residues toward the bilayer. After 10 ns, the entire Aβ dimer is rolled over by ∼82°,

DOI: 10.1021/acs.biochem.5b00719
Biochemistry 2015, 54, 6323−6332

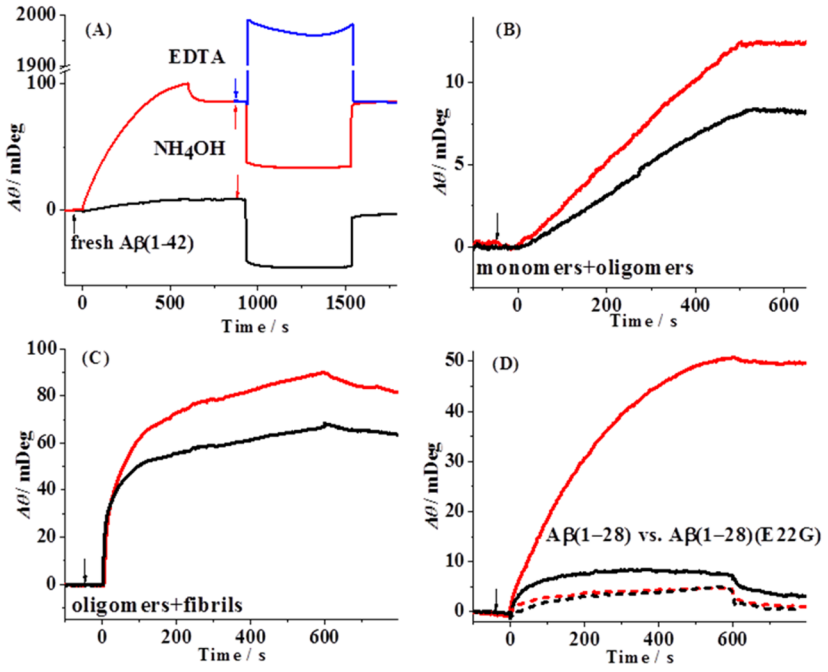

Figure 2. SPR sensorgrams showing the interaction between supported DPPS bilayers and various Aβ species in the presence (red curves) and absence of 10 mM Ca^{2+} (curves in black): (A) Aβ(1−42) monomers/dimers in freshly prepared Aβ(1−42) solutions, with the red arrows indicating the injections of 1% NH_4OH and the blue arrow the injection of 0.5 M EDTA, (B) Aβ(1−42) monomers/various oligomers in an Aβ(1−42) solution that had been preincubated for 3 h, (C) oligomers/fibrils in an Aβ(1−42) solution that had been preincubated for 6 h, and (D) Aβ(1−28) and the Aβ(1−28)(E22G) mutant (solid and dashed curves, respectively). All Aβ solutions had an initial concentration of 12.5 μM and the black arrows indicate the injections of the Aβ samples.

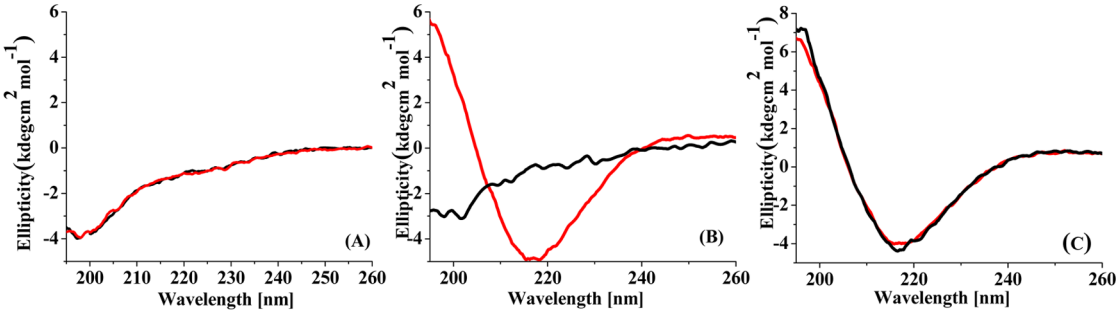

Figure 3. CD spectra of 25 μM Aβ(1−42) in the presence of 0.5 mM Ca^{2+} (A), 1 mg/mL DPPS vesicles (B), and 0.5 mM Ca^{2+} and 1 mg/mL DPPS vesicles (C). The black and red curves correspond to the same Aβ(1−42) solution incubated for 0 and 6 h, respectively.

completely changing its orientation from the initial β-hairpin to an arrangement in which the N-terminal residues are in contact with the bilayer. The new orientation remains unchanged until the end of the 20 ns simulation. The Aβ dimer structure at the DPPS bilayer is analogous to that in solution, although the flexibility of the former is more restricted. Our simulation also reveals that during the adsorption process, Ca^{2+} ions (shown as gray spheres in Figure 1) are in close vincinity of both the negatively charged Glu-22 residue of the Aβ peptide and the phosphate groups on the DPPS molecules. Clearly, in the stable configuration (15 ns and later), both the N- and C-termini are well exposed to solution above the lipid bilayer.

Surface plasmon resonance (SPR) has been demonstrated as a viable technique for studying Aβ adsorption onto lipid bilayers and the interaction between Aβ and drug candidates.[30,58] We used it in this work to determine the Ca^{2+} effect on the adsorption of Aβ peptides onto lipid bilayers. In the presence of Ca^{2+} (red curve in Figure 2A), at 12.5 μM, Aβ(1−42) molecules adsorbed on a supported DPPS bilayer are 9 fold greater than those in the absence of Ca^{2+} (black curve). NH_4OH is known to cause a disruption of the structure of lipid bilayer.[59,60] After 1% NH_4OH was introduced into the SPR channels, Aβ(1−42) adsorbed in the absence of Ca^{2+} can be completely desorbed, as evidenced by the recovery of the signal to the original baseline after the NH_4OH elution. The inverted injection peak is due to change in the bulk refractive index when NH_4OH entered the SPR channel. Interestingly, Aβ(1−42) molecules attached in the presence of Ca^{2+} remains on the surface (i.e., no net change in the baseline of the red curve after the NH_4OH elution). The fact that Aβ(1−42) is not detached from the DPPS bilayer indicates that, as predicted by our MD calculation, Ca^{2+} is key to the retention of the Aβ(1−42) molecules by the lipid bilayers. In a separate experiment, 0.5 M EDTA was injected, which produced an upward injection peak (blue curve; due to an increase in the bulk refractive index) but still returned to the original baseline after the EDTA elution. Thus, the interaction among Aβ(1−42), Ca^{2+} and lipid is quite strong. As a result, under the experimental condition Ca^{2+} ions

DOI: 10.1021/acs.biochem.5b00719
Biochemistry 2015, 54, 6323−6332

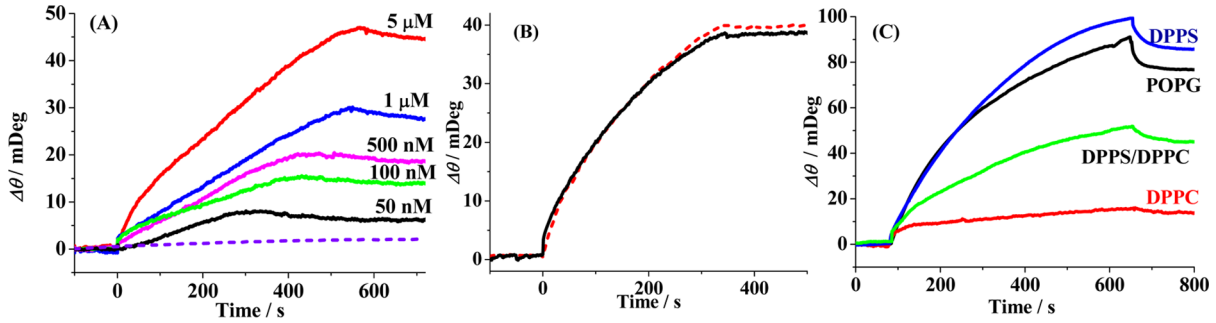

Figure 4. SPR sensorgrams showing (A) the attachment of Aβ(1−42) onto DPPS bilayers from artificial CSF solutions containing different Aβ(1−42) concentrations (50 nM−5 μM) in the presence of 10 mM Ca^{2+} and the behavior of 5 μM Aβ(1−42) in the absence of Ca^{2+} (dotted curve), (B) the attachments of Aβ(1−42) C-terminus antibody (black curve) and N-terminus antibody (red) onto Aβ(1−42) preadsorbed at DPPS bilayers in the presence of 10 mM Ca^{2+}, and (C) the attachments of Aβ(1−42) from phosphate buffer containing 12.5 μM Aβ(1−42) onto DPPS (blue curve), POPG (black curve), DPPC (red curve), and 1:1 (V:V) mixed DPPS/DPPC bilayers (green curve).

are not sequestered by EDTA flowing over the surface. When Aβ(1−42) monomer/oligomers (Figure 2B) or oligomers/fibril (Figure 2C) were introduced, a similar Ca^{2+} effect was also observed. We did not observe the above effects when Ca^{2+} was replaced with Mg^{2+}. We also found that decreasing the Ca^{2+} concentration from 50 to 0.5 mM did not change the SPR responses shown in Figure 2. Since our MD calculation predicts that Glu-22 is essential for the Ca^{2+}binding to Aβ(1−42), we used the Aβ(1−28)(E22G) mutant to perform another SPR experiment. As shown by the red and black dashed curves in Figure 2D, the Ca^{2+} effect was completely abolished as few Aβ(1−28)(E22G) mutants were attached to the DPPS bilayer. In contrast, when Aβ(1−28) was used, Ca^{2+} leads to much greater Aβ(1−28) adsorption (cf. Figure 2D solid red line), a trend analogous to that in Figure 2A. We chose to compare Aβ(1−28) to its E22G mutant because synthesis of Aβ(1−42) with the E22G mutation is time-consuming and of low yield. On the basis of the facts that (1) 1−28 segment encompasses Glu-22, (2) the Ca^{2+} effect is evident from the stark contrast between solid curves in Figure 2D, and (3) Aβ(1−28) induces behaviorial changes in rats[48,49] similarly to Aβ(1−40), Aβ(1−28) and its mutant are applicable.

We next assessed whether the presence of Ca^{2+} and/or DPPS bilayers promotes a change in the Aβ(1−42) secondary structure. In the presence of Ca^{2+}, the circular dichroism (CD) spectrum of Aβ(1−42) freshly dissolved in artificial CSF (black curve in Figure 3A) exhibits the natively unstructured conformation, as evidenced by the characteristic peak at 197 nm. This peak gradually disappears after 6 h (red curve). In the presence of DPPS vesicles (Figure 3B), this peak disappears much more rapidly and is converted into the peak characteristic of the β-sheet structure (217 nm in the red curve) after 6 h of incubation. Thus, consistent with other reports,[61,62] Aβ(1−42) indeed aggregates faster in the presence of lipid bilayers. Most dramatically, when both DPPS and Ca^{2+} are present in solution, the natively unstructured conformation of Aβ(1−42) was not even observable at the beginning of the incubation (Figure 3C). Thus, Ca^{2+} and DPPS bilayers concertedly promote the rapid β-sheet formation (i.e., dimerization and oligomerization) of Aβ(1−42).

To investigate whether the observed Ca^{2+} effect enhances accumulation of Aβ(1−42) at lipid bilayers under conditions similar to the physiological milieu, we injected artificial CSF solutions containing a series of Aβ(1−42) concentrations that are all well below the CMC (Figure 4A). As can be seen, even at 50 nM (black curve), a concentration close to that in CSF (0.6−10 nM),[14−18] an easily discernible Aβ(1−42) adsorption signal was observed. In the absence of Ca^{2+}, no signal was observable even at 5 μM Aβ(1−42) (cf. dotted line curve). The binding constant (K_D) was estimated to be 229.1 ± 1.0 nM^{-1}. We also monitored the attachments of the Aβ(1−42) C- and N-terminus-specific antibodies. Clearly from Figure 4B, Aβ(1−42) molecules attached to the DPPS bilayers via Ca^{2+} are recognized by both types of antibodies. This result suggests that the Aβ(1−42) molecules are anchored to the DPPS bilayer with their C- and N- termini well exposed to the solution. Thus, Ca^{2+} is essential in decreasing the repulsion between the lipid headgroups and the negatively charged residues of Aβ(1−42). The exposed Aβ(1−42) C- and N-termini are consistent with the configuration or positioning of the dimers at the lipid bilayer revealed by our MD calculation (cf. Figure 1). We should add that the dimer considered by the MD calculation is Aβ(17−42). In other words, the first 16 residues of Aβ(1−42) were excluded due to the reasons delineated for the MD calculation (cf. Materials and Methods). However, given that Aβ(1−16) is hydrophilic and known to not insert into the lipid bilayer,[63] it is not surprising that the N-terminus of Aβ(1−42) was found to be exposed to solution. We further investigated the effects of the charges on the lipid head groups, saturation of the lipid hydrocarbon chain, and bilayer composition on the amount of Aβ(1−42) attachment. As can be seen from Figure 4C, the amount of Aβ(1−42) attachment onto the bilayer of POPG (black curve), an unsaturated phospholipid that resembles more closely to neuronal membrane, is comparable to that onto the DPPS bilayer (blue curve). This result suggests that, as long as the glycerol side-chain on the lipid head is neutral, the amount of Aβ(1−42) attachment in the presence of Ca^{2+} is largely independent of the saturation of the phospholipid hydrophobic chain. Interestingly, if the glycerol side-chain is positively charged (as in the case of DPPC), the amount of Aβ(1−42) attachment is significantly reduced (red curve). We think that the positively charged amine group probably repels Ca^{2+} and weakens the interaction of Ca^{2+} with Aβ(1−42) and the lipid bilayer. It is also apparent from Figure 4C that Ca^{2+} leads to Aβ(1−42) attachment to the mixed DPPS/DPPC (1:1) bilayer (green curve), a situation analogous to the composition of neuronal membrane.

Finally, we conducted time-lapse AFM to image species adsorbed onto a DPPS bilayer in an artificial CSF solution containing a low Aβ(1−42) concentration (0.5 μM). AFM can only image oligomers of a few nanometers in diameter (typically pentamers or higher[22,64,65]). In the presence of

DOI: 10.1021/acs.biochem.5b00719
Biochemistry 2015, 54, 6323−6332

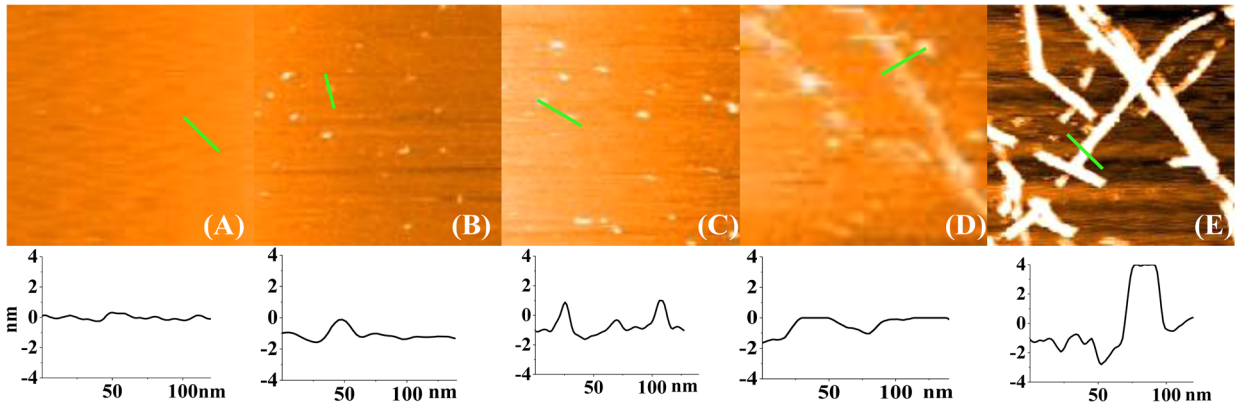

Figure 5. Time-lapse AFM images (250 nm × 250 nm) showing oligomerization/fibrillation of 0.5 μM Aβ(1−42) at DPPS bilayers in aCSF at (A) 0 h, (B) 24 h, (C) 48 h, and (D) 72 h. Preformed fibrils attached to DPPS bilayers are shown in (E). Cross-sectional contours of representative oligomers and fibrils, denoted by green bars in the images, are shown below the images.

Ca^{2+}, oligomers with diameters ranging from 10 to 60 nm were observed after 24 h of incubation (cf. Figure 5B and the cross-sectional contour). These oligomers grew into larger ones after 48 h (cf. Figure 5C and the cross-sectional contour). After incubation for 72 h, fibrils as long as 1.2 μm were formed (Figure 5D). Without Ca^{2+}, the AFM images (data not shown) are essentially the same as that shown in Figure 5A, indicating neither globular oligomers nor fibrils were formed during the same timeframes. To exclude the possibility that oligomers and fibrils are initially formed in solution and subsequently deposited onto the lipid bilayer, we performed thioflavin-T fluorescence assay in an artifical CSF solution containing 0.5 μM Aβ(1−42) and 1.4 mM Ca^{2+} and found no enhanced fluorescence signal. This is not surprising as 0.5 μM is well below the CMC for Aβ(1−42) to aggregate in a lipid-free solution. We also discovered that Aβ(1−42) fibrils preformed at a high concentration (25 μM) and subsequently deposited onto DPPS bilayers (Figure 5E) appear to "protrude" from the bilayer surface when compared to those grown on the bilayers in the presence of Ca^{2+}. Because the Aβ(1−42) molecules are anchored to the phospholipid bilayers via Ca^{2+} ions, the observed oligomers and fibrils (cf. Figure 5D) have higher fluidity. Consequently, the AFM image is less well-defined due to the AFM tip "broadening effect"[66] when compared to fibrils preformed in solution and subsequently deposited onto the bilayers (cf. Figure 5E). Therefore, it is clear that at low Aβ(1−42) concentrations, Aβ(1−42) aggregation or fibrillation does not occur at a noticeable rate without Ca^{2+} and the DPPS bilayer. This finding is consistent with our aformentioned computational and experimental data.

DISCUSSION

Mounting evidence has linked calcium dyshomeostasis to neuropathology of AD.[34,35,67] In some reports disruption of calcium signaling is shown to occur before the Aβ production,[19,68] but in other studies modulation of the APP metabolism or damage of cell membrane by aggregated Aβ is suggested to affect the calcium level in the cytoplasm.[35,68] Calcium in the neuronal cytosol is at the nanomolar level, which is much lower than that in the extracellular space (~2−10 mM[34,69]) and bloodstream (~2.5 mM[70]) where more than 50% of Ca^{2+} ions are free, while the rest are bound by proteins, hormones, and small anions.[71] It is well-known that Ca^{2+} has a strong affinity for phosphate ions, as evidenced by calcium storage as a phosphate salt or precipitate inside cells.[71] Surprisingly, studies on the interaction between Aβ and lipid bilayer or cell membrane have largely overlooked the effect of Ca^{2+} on the initial adsorption and subsequent accumulation of Aβ peptides at phospholipids, even though such an effect has been noted in the studies of other amyloidogenic species such as IAPP and α-synuclein.[40,41] Our SPR data suggest that Ca^{2+} not only strengthens the interaction between Aβ peptides and phospholipids (Figure 2A) but also helps scavenge trace amounts of Aβ molecules at the lipid/solution interface to accelerate Aβ oligomerization/fibrillation (Figure 4A). These functions are unique of Ca^{2+}, as Mg^{2+} does not hasten the Aβ adsorption/oligomerization. A similar trend has been reported by Narayanaswami and co-workers on α-synuclein.[41] It is well-known that outside the cell membrane a thin, nanometer-sized solution layer exists whose dielectric constant is 10 times less than that of the extracellular matrix.[20,32,72,73] Such a situation is also applicable to the lipid bilayer/solution interface. The substantially decreased dielectric constant facilitates the conversion of the unstructured Aβ(1−42) monomers to β-sheet-containing structures such as dimers. Such structures, once anchored by Ca^{2+} onto lipids, can serve as nuclei for further interaction with other Aβ molecules in solution.[74] Indeed, our CD spectra confirmed that Aβ(1−42) readily undergoes the transformation from the unstructured conformation to β-sheets at the lipid bilayer/solution interface (Figure 3C). In parallel, we used MD simulations to study the interaction of Aβ dimer with lipid bilayers. We chose Aβ dimer for our MD calculation on the basis that (1) it is the smallest and earliest oligomer with a β-sheet and (2) only Aβ monomer and dimer are believed to be able to insert into the cell membrane,[26,33,75] and (3) dimers, along with other small and diffusible oligomers, are most cytotoxic.[76] Our calculation suggests that, when Ca^{2+} is present, at the lipid bilayer the dimer adopts an orientation in which the C- and N-termini are fully exposed to solution (Figure 1). Such exposures were confirmed by our SPR experiments (Figure 4B). Although membrane disruption induced by Aβ in the presence of Ca^{2+} was not observed within the short MD time scale, Ca^{2+} enhances the Aβ accumulation to ultimately affect the integrity of cell membrane. The similar orientation of the negatively charged C-terminus of α-synuclein to the phospholipids via the "Ca^{2+} bridge" also supports our finding.[41] Oligomers and fibrils formed in the presence of Ca^{2+} appear to be fluid at the lipid bilayer (Figure 5D), contrary to those deposited from solution,

DOI: 10.1021/acs.biochem.5b00719
Biochemistry 2015, 54, 6323−6332

which are firmly stacked on top of the bilayer (Figure 5E). Although our study centers on the effect of Ca^{2+} on the initial adsorption of Aβ at lipid bilayers, the results suggest that any oligomers and fibrils attached to membrane via Ca^{2+} might affect more adversely the integrity of neurons[77] than their counterparts preformed in solution.

With the Ca^{2+}-anchored Aβ molecules serving as nuclei, Aβ aggregation can occur at the lipid bilayer at exceedingly low concentrations (Figure 4A). Without Ca^{2+} as an additive, Ding et al.[19] and Nag et al.[21] have used single molecule spectroscopy to detect Aβ adsorption at 100−150 nM at the lipid bilayer and PC12 cells, respectively. The detection limit of our and other SPR instruments is about 10 fg/cm^2 or approximately 10^5 molecules/cm^2,[45,78] far lower than the sensitivity of single molecule spectroscopy.[79] Yet we were able to detect the adsorption of Aβ(1−42) at a concentration as low as 50 nM, a value more than 2 orders of magnitude lower than the Aβ(1−42) CMC. Our data therefore suggest that Ca^{2+} plays a pivotal role in the initial Aβ adsorption for lowering the concentration needed for Aβ nucleation at lipid surfaces. The critical concentration needed for fibril formation was calculated to be on the order of 10 nM by their model.[80] At 2 nM, a concentration within the range of Aβ found in CSF,[15,16] single molecule spectroscopy detected Aβ at PC12 cells after 1 week,[21] suggesting that the initial adsorption of Aβ molecules is an extremely slow process. In the presence of Ca^{2+}, it is likely that this process will be accelerated.

Although our study does not sort the order of sequence between calcium dyshomeostasis and Aβ formation/aggregation, it is evident that these two events are intricately related. On the one hand, any elevation of free Ca^{2+} near neuronal cell membrane will speed up the Aβ attachment and aggregation. On the other hand, Aβ aggregates impair the membrane, disrupting the Ca^{2+} flux. In CSFs of AD patients, both the calcium and phosphorus levels are decreased by almost 50% with respect to those of age-matched controls.[81] In contrast, in serum samples such decreases are marginal. The Ca × P product was used as a possible criterion for calcium deposition (one aspect of calcium dyshomeostasis) in the AD brain.[81] Thus, once Aβ is cleaved from APP through a Ca^{2+}-dyshomeostasis-triggered cascade or even through a Ca^{2+}-independent pathway, the attachment of Aβ onto neuronal cell membrane is likely to take place given the large Ca^{2+} concentrations outside the neuronal cells.

Finally, it is well accepted that Aβ oligomers cannot penetrate membranes, and only the C-terminus of Aβ monomers or dimers can insert into membranes.[82,83] Different and somewhat conflicting models have been proposed regarding the interaction of the various Aβ species with membranes. For example, based on MD calculations, Tofoleanu and Buchete suggested that the 1−28 segment of Aβ, specifically with residues Glu-22, Asp-23, and Lys-28, is key to initial electrostatic interaction between the Aβ monomer and the lipid headgroups.[28] The interior of the lipid bilayers facilitates the insertion of the Aβ C-terminus into membrane to attenuate electrostatic repulsion. On a longer time scale, the Aβ monomer may adopt a largely helical structure inside the membrane.[28] Pannuzzo et al. performed multiscale coarse-grained and atomistic MD simulations to study the interaction of Aβ(1−40) with the POPC bilayer in the microsecond domain. They found that as Aβ peptides adsorbed and aggregated at the POPC bilayer, an obvious membrane curvature was induced with the Aβ helical structure maintained in the aggregated form. This suggests that a conformational transition from the helical structure to a β-sheet-rich structure could be a prerequisite step for membrane damage.[84] Interestingly, without the consideration of the Ca^{2+} effect, Glu-22 and Asp-23 disfavor the attachment of Aβ onto negatively charged lipids, whereas Lys-28 accommodates electrostatic attraction. If the Ca^{2+} effect was considered, the opposite would hold true. Particularly relevant to our work is the mechanism reported by Cohen et al. on the fibril-catalyzed oligomer formation.[80] The work demonstrated that, in the presence of a small amount of fibrils, rapid production of Aβ oligomers from solutions containing as low as 10 nM Aβ monomer is possible. From Figure 5, it is apparent that fibrils can be formed at lipid surfaces at low Aβ concentration in the presence of Ca^{2+}, and the fibril-accelerated conversion of monomers into cytotoxic oligomers can ultimately lead to membrane damage.[9] Recently, Xiong et al.[82] suggest that insertion of Aβ(1−40) into lipid bilayers is followed by a conversion into the β-sheet structure, which forces the C-terminus out of the membrane for incorporating additional Aβ(1−40) molecules. However, in the presence of Ca^{2+}, the C-terminus is stabilized and does not need to insert into the lipids to maximize the hydrophobic interaction or decrease the electrostatic repulsion. Thus, studies on the electrostatic and hydrophobic interactions between Aβ and lipids might not be comprehensive without taking into account the role of Ca^{2+} in the initial adsorption of Aβ molecules. It should be meaningful to revisit some of these models in the context of the Ca^{2+} effect.

■ CONCLUSIONS

We present experimental and computational results that clearly demonstrate the important role of Ca^{2+} in the initial attachment and subsequent accumulation of Aβ peptides at the phospolipid surface. The interaction among Ca^{2+}, Glu-22 of Aβ, and the phosphate group on the phospholipid bilayer is quite strong, and the Ca^{2+}-anchored Aβ dimers adopt an orientation in which both N- and C-termini are spatially accessible to additional Aβ molecules and antibodies. This biologically relevant finding helps explain why in vivo aggregation of Aβ peptides occurs at concentrations that are substantially lower than that observed in vitro. Our results also suggest that future studies about Aβ aggregation at membranes should take into account the premise of the calcium hypothesis in general and the Ca^{2+} effect reported herein in particular.

■ AUTHOR INFORMATION

Corresponding Authors

*E-mail: zhengj@uakron.edu.
*E-mail: fzhou@calstatela.edu.

Author Contributions

X.Y. and Y.Z. performed the SPR experiments, X.Y. and M.G. performed the AFM measurements, X.Y. collected the CD spectra, N.D. synthesized peptides, X.Y. and J.Z. conducted the MD simulation, J.Z. directed the research with F.Z., and F.Z. wrote the manuscript.

Funding

This work was supported by the National Institutes of Health (R01-GM105898), the National Key Basic Research Program of China (2014CB744502), a 2011 Collaborative and Innovative Grant from Hunan Province of China and the National Science Foundation (No. 1112105 for F.Z. and CBET-0952624 and CBET115844 for J.Z.).

DOI: 10.1021/acs.biochem.5b00719
Biochemistry 2015, 54, 6323−6332

Notes

The authors declare no competing financial interest.

■ ACKNOWLEDGMENTS

We thank the anonymous reviewers for their comments and for suggesting additional experiments to examine the Ca^{2+} effect at different lipids.

■ ABBREVIATIONS

AD: Alzheimer's disease; Aβ: amyloid beta; CMC: critical micelle concentration; CSF: cerebrospinal fluid; aCSF: artificial cerebrospinal fluid; AFM: atomic force microscopy; CD: circular dichroism; SPR: surface plasmon resonance; R_t: retention time; MD: molecular dynamics; DPPS: 1, 2-dipalmitoyl-*sn*-glycero-3-phospho-L-serine; DPPC: 1,2-dipalmitoyl-*sn*-glycero-3-phosphocholine; POPG: 1-palmitoyl-2-oleoyl-*sn*-glycero-3-phospho-1′-*rac*-glycerol; POPC: 1-palmitoyl-2-oleoyl-*sn*-glycero-3-phosphocholine

■ REFERENCES

(1) Hardy, J., and Selkoe, D. J. (2002) Medicine - The amyloid hypothesis of Alzheimer's disease: progress and problems on the road to therapeutics. *Science 297*, 353−356.

(2) Kang, J., Lemaire, H. G., Unterbeck, A., Salbaum, J. M., Masters, C. L., Grzeschik, K. H., Multhaup, G., Beyreuther, K., and Muller-Hill, B. (1987) The precursor of Alzheimer's disease amyloid A4 protein resembles a cell-surface receptor. *Nature 325*, 733−736.

(3) Selkoe, D. J. (1997) Alzheimer's disease: genotypes, phenotypes, and treatments. *Science 275*, 630−631.

(4) Strodel, B., Lee, J. W. L., Whittleston, C. S., and Wales, D. J. (2010) Transmembrane structures for Alzheimer's abeta(1−42) oligomers. *J. Am. Chem. Soc. 132*, 13300−13312.

(5) Bucciantini, M., Giannoni, E., Chiti, F., Baroni, F., Formigli, L., Zurdo, J. S., Taddei, N., Ramponi, G., Dobson, C. M., and Stefani, M. (2002) Inherent toxicity of aggregates implies a common mechanism for protein misfolding diseases. *Nature 416*, 507−511.

(6) Iversen, L. L., Mortishire-Smith, R. J., Pollack, S. J., and Shearman, M. S. (1995) The toxicity in vitro of beta-amyloid protein. *Biochem. J. 311* (1), 1−16.

(7) Lansbury, P. T. (1999) Evolution of amyloid: What normal protein folding may tell us about fibrillogenesis and disease. *Proc. Natl. Acad. Sci. U. S. A. 96*, 3342−3344.

(8) Rochet, J. C., and Lansbury, P. T. (2000) Amyloid fibrillogenesis: themes and variations. *Curr. Opin. Struct. Biol. 10*, 60−68.

(9) Kayed, R., Sokolov, Y., Edmonds, B., McIntire, T. M., Milton, S. C., Hall, J. E., and Glabe, C. G. (2004) Permeabilization of lipid bilayers is a common conformation-dependent activity of soluble amyloid oligomers in protein misfolding diseases. *J. Biol. Chem. 279*, 46363−46366.

(10) Kirkitadze, M. D., Condron, M. M., and Teplow, D. B. (2001) Identification and characterization of key kinetic intermediates in amyloid beta-protein fibrillogenesis. *J. Mol. Biol. 312*, 1103−1119.

(11) Harper, J. D., and Lansbury, P. T., Jr. (1997) Models of amyloid seeding in Alzheimer's disease and scrapie: mechanistic truths and physiological consequences of the time-dependent solubility of amyloid proteins. *Annu. Rev. Biochem. 66*, 385−407.

(12) Lomakin, A., Chung, D. S., Benedek, G. B., Kirschner, D. A., and Teplow, D. B. (1996) On the nucleation and growth of amyloid beta-protein fibrils: detection of nuclei and quantitation of rate constants. *Proc. Natl. Acad. Sci. U. S. A. 93*, 1125−1129.

(13) Sabate, R., and Estelrich, J. (2005) Evidence of the existence of micelles in the fibrillogenesis of beta-amyloid peptide. *J. Phys. Chem. B 109*, 11027−11032.

(14) Haass, C., Schlossmacher, M. G., Hung, A. Y., Vigo-Pelfrey, C., Mellon, A., Ostaszewski, B. L., Lieberburg, I., Koo, E. H., Schenk, D., Teplow, D. B., and Selkoe, D. J. (1992) Amyloid beta-peptide is produced by cultured cells during normal metabolism. *Nature 359*, 322−325.

(15) Seubert, P., Vigo-Pelfrey, C., Esch, F., Lee, M., Dovey, H., Davis, D., Sinha, S., Schiossmacher, M., Whaley, J., Swindlehurst, C., McCormack, R., Wolfert, R., Selkoe, D., Lieberburg, I., and Schenk, D. (1992) Isolation and quantification of soluble Alzheimer's beta-peptide from biological fluids. *Nature 359*, 325−327.

(16) Shoji, M., Golde, T. E., Ghiso, J., Cheung, T. T., Estus, S., Shaffer, L. M., Cai, X. D., McKay, D. M., Tintner, R., Frangione, B., et al. (1992) Production of the Alzheimer amyloid beta protein by normal proteolytic processing. *Science 258*, 126−129.

(17) Southwick, P. C., Yamagata, S. K., Echols, C. L., Jr., Higson, G. J., Neynaber, S. A., Parson, R. E., and Munroe, W. A. (1996) Assessment of amyloid beta protein in cerebrospinal fluid as an aid in the diagnosis of Alzheimer's disease. *J. Neurochem. 66*, 259−265.

(18) Wang, R., Sweeney, D., Gandy, S. E., and Sisodia, S. S. (1996) The profile of soluble amyloid beta protein in cultured cell media: detection and quantification of amyloid beta protein and variants by immunoprecipitation-mass spectrometry. *J. Biol. Chem. 271*, 31894−31902.

(19) Ding, H., Schauerte, J. A., Steel, D. G., and Gafni, A. (2012) Beta-Amyloid (1−40) peptide interactions with supported phospholipid membranes: a single-molecule study. *Biophys. J. 103*, 1500−1509.

(20) Jiang, D., Dinh, K. L., Ruthenburg, T. C., Zhang, Y., Su, L., Land, D. P., and Zhou, F. (2009) A kinetic model for beta-amyloid adsorption at the air/solution interface and its implication to the beta-amyloid aggregation process. *J. Phys. Chem. B 113*, 3160−3168.

(21) Nag, S., Chen, J., Irudayaraj, J., and Maiti, S. (2010) Measurement of the attachment and assembly of small amyloid-beta oligomers on live cell membranes at physiological concentrations using single-molecule tools. *Biophys. J. 99*, 1969−1975.

(22) Kowalewski, T., and Holtzman, D. M. (1999) In situ atomic force microscopy study of Alzheimer's beta-amyloid peptide on different substrates: new insights into mechanism of beta-sheet formation. *Proc. Natl. Acad. Sci. U. S. A. 96*, 3688−3693.

(23) Yamaguchi, H., Maat-Schieman, M. L. C., van Duinen, S. G., Prins, F. A., Neeskens, P., Natte, R., and Roos, R. A. C. (2000) Amyloid beta protein (A beta) starts to deposit as plasma membrane-bound form in diffuse plaques of brains from hereditary cerebral hemorrhage with amyloidosis-Dutch type, Alzheimer disease and nondemented aged subjects. *J. Neuropathol. Exp. Neurol. 59*, 723−732.

(24) Yip, C. M., Darabie, A. A., and McLaurin, J. (2002) Abeta 42-peptide assembly on lipid bilayers. *J. Mol. Biol. 318*, 97−107.

(25) Sokolov, Y. V., Kayed, R., Kozak, A., Edmonds, B., McIntire, T. M., Milton, S., Cahalan, M., Glabe, C. G., and Hall, J. E. (2004) Soluble amyloid oligomers increase lipid bilayer conductance by increasing the dielectric constant of the hydrocarbon core. *Biophys. J. 86*, 382A−382A.

(26) Valincius, G., Heinrich, F., Budvytyte, R., Vanderah, D. J., McGillivray, D. J., Sokolov, Y., Hall, J. E., and Losche, M. (2008) Soluble amyloid beta-oligomers affect dielectric membrane properties by bilayer insertion and domain formation: implications for cell toxicity. *Biophys. J. 95*, 4845−4861.

(27) Bokvist, M., Lindstrom, F., Watts, A., and Grobner, G. (2004) Two types of Alzheimer's beta-amyloid (1−40) peptide membrane interactions: Aggregation preventing transmembrane anchoring versus accelerated surface fibril formation. *J. Mol. Biol. 335*, 1039−1049.

(28) Tofoleanu, F., and Buchete, N.-V. (2012) Molecular interactions of Alzheimer's abeta protofilaments with lipid membranes. *J. Mol. Biol. 421*, 572−586.

(29) Bokvist, M., and Grobner, G. (2007) Misfolding of amyloidogenic proteins at membrane surfaces: The impact of macromolecular crowding. *J. Am. Chem. Soc. 129*, 14848−14849.

(30) Kremer, J. J., and Murphy, R. M. (2003) Kinetics of adsorption of β-amyloid peptide Aβ(1−40) to lipid bilayers. *J. Biochem. Biophys. Methods 57*, 159−169.

(31) Terzi, E., Holzemann, G., and Seelig, J. (1997) Interaction of Alzheimer beta-amyloid peptide(1−40) with lipid membranes. *Biochemistry 36*, 14845−14852.

DOI: 10.1021/acs.biochem.5b00719
Biochemistry 2015, 54, 6323−6332

(32) Chi, E. Y., Ege, C., Winans, A., Majewski, J., Wu, G., Kjaer, K., and Lee, K. Y. C. (2008) Lipid membrane templates the ordering and induces the fibrillogenesis of Alzheimer's disease amyloid-beta peptide. *Proteins: Struct., Funct., Genet. 72*, 1−24.
(33) Wong, P. T., Schauerte, J. A., Wisser, K. C., Ding, H., Lee, E. L., Steel, D. G., and Gafni, A. (2009) Amyloid-beta membrane binding and permeabilization are distinct processes influenced separately by membrane charge and fluidity. *J. Mol. Biol. 386*, 81−96.
(34) LaFerla, F. M. (2002) Calcium dyshomeostasis and intracellular signalling in Alzheimer's disease. *Nat. Rev. Neurosci. 3*, 862−872.
(35) Mattson, M. P., and Chan, S. L. (2003) Neuronal and glial calcium signaling in Alzheimer's disease. *Cell Calcium 34*, 385−397.
(36) Disterhoft, J. F., Moyer, J. R., Jr., and Thompson, L. T. (1994) The calcium rationale in aging and Alzheimer's disease: Evidence from an animal model of normal aging. *Ann. N. Y. Acad. Sci. 747*, 382−406.
(37) Querfurth, H. W., and Selkoe, D. J. (1994) Calcium ionophore increases amyloid beta peptide production by cultured cells. *Biochemistry 33*, 4550−4561.
(38) Leissring, M. A., Murphy, M. P., Mead, T. R., Akbari, Y., Sugarman, M. C., Jannatipour, M., Anliker, B., Muller, U., Saftig, P., De Strooper, B., Wolfe, M. S., Golde, T. E., and LaFerla, F. M. (2002) A physiologic signaling role for the gamma-secretase-derived intracellular fragment of APP. *Proc. Natl. Acad. Sci. U. S. A. 99*, 4697−4702.
(39) Mattson, M. P., Cheng, B., Davis, D., Bryant, K., Lieberburg, I., and Rydel, R. E. (1992) Beta-Amyloid peptides destabilize calcium homeostasis and render human cortical neurons vulnerable to excitotoxicity. *J. Neurosci. 12*, 376−389.
(40) Sciacca, M. F. M., Milardi, D., Messina, G. M. L., Marletta, G., Brender, J. R., Ramamoorthy, A., and La Rosa, C. (2013) Cations as switches of amyloid-mediated membrane disruption mechanisms: calcium and IAPP. *Biophys. J. 104*, 173−184.
(41) Tamamizu-Kato, S., Kosaraju, M. G., Kato, H., Raussens, V., Ruysschaert, J. M., and Narayanaswami, V. (2006) Calcium-triggered membrane interaction of the alpha-synuclein acidic tail. *Biochemistry 45*, 10947−10956.
(42) Sciacca, M. F., Pappalardo, M., Milardi, D., Grasso, D. M., and La Rosa, C. (2008) Calcium-activated membrane interaction of the islet amyloid polypeptide: implications in the pathogenesis of type II diabetes mellitus. *Arch. Biochem. Biophys. 477*, 291−298.
(43) Yu, X., and Zheng, J. (2012) Cholesterol promotes the interaction of Alzheimer beta-amyloid monomer with lipid bilayer. *J. Mol. Biol. 421*, 561−571.
(44) Mou, J. X., Czajkowsky, D. M., and Shao, Z. F. (1996) Gramicidin A aggregation in supported gel state phosphatidylcholine bilayers. *Biochemistry 35*, 3222−3226.
(45) Yi, X., Hao, Y., Xia, N., Wang, J., Quintero, M., Li, D., and Zhou, F. (2013) Sensitive and continuous screening of inhibitors of beta-site amyloid precursor protein cleaving enzyme 1 (BACE1) at single SPR chips. *Anal. Chem. 85*, 3660−3666.
(46) Luhrs, T., Ritter, C., Adrian, M., Riek-Loher, D., Bohrmann, B., Dobeli, H., Schubert, D., and Riek, R. (2005) 3D structure of Alzheimer's amyloid-beta(1−42) fibrils. *Proc. Natl. Acad. Sci. U. S. A. 102*, 17342−17347.
(47) Paravastu, A. K., Leapman, R. D., Yau, W.-M., and Tycko, R. (2008) Molecular structural basis for polymorphism in Alzheimer's beta-amyloid fibrils. *Proc. Natl. Acad. Sci. U. S. A. 105*, 18349−18354.
(48) Alvarez, X. A., Miguel-Hidalgo, J. J., Fernández-Novoa, L., and Cacabelos, R. (1997) Intrahippocampal injections of the beta-amyloid 1−28 fragment induces behavioral deficits in rats. *Methods Find. Exp. Clin. Pharmacol. 19*, 471−479.
(49) Koudinov, A. R., Koudinova, N. V., and Berezov, T. T. (1996) Alzheimer's peptides abeta 1−40 and abeta 1−28 inhibit the plasma cholesterol esterification rate. *Biochem. Mol. Biol. Int. 38*, 747−752.
(50) Miller, Y., Ma, B., and Nussinov, R. (2009) Polymorphism of Alzheimer's abeta17−42 (p3) oligomers: the importance of the turn location and its conformation. *Biophys. J. 97*, 1168−1177.
(51) Schneidman-Duhovny, D., Inbar, Y., Nussinov, R., and Wolfson, H. J. (2005) PatchDock and SymmDock: Servers for rigid and symmetric docking. *Nucleic Acids Res. 33*, w363−w367.
(52) Mashiach, E., Schneidman-Duhovny, D., Andrusier, N., Nussinov, R., and Wolfson, H. J. (2008) FireDock: a web server for fast interaction refinement in molecular docking. *Nucleic Acids Res. 36*, w229−w232.
(53) Jo, S., Lim, J. B., Klauda, J. B., and Im, W. (2009) CHARMM-GUI membrane builder for mixed bilayers and its application to yeast membranes. *Biophys. J. 97*, 50−58.
(54) Yu, X., Wang, Q., Pan, Q., Zhou, F., and Zheng, J. (2013) Molecular interactions of Alzheimer amyloid-beta oligomers with neutral and negatively charged lipid bilayers. *Phys. Chem. Chem. Phys. 15*, 8878−8889.
(55) Ciudad, D. (2015) Going electric. *Nat. Mater. 14*, 134−134.
(56) O'Malley, T. T., Oktaviani, N. A., Zhang, D., Lomakin, A., O'Nuallain, B., Linse, S., Benedek, G. B., Rowan, M. J., Mulder, F. A. A., and Walsh, D. M. (2014) Abeta dimers differ from monomers in structural propensity, aggregation paths and population of synaptotoxic assemblies. *Biochem. J. 461*, 413−426.
(57) Zhang, T., Xu, W., Mu, Y., and Derreumaux, P. (2014) Atomic and dynamic insights into the beneficial effect of the 1,4-naphthoquinon-2-yl-L-tryptophan inhibitor on Alzheimer's abeta 1−42 dimer in terms of aggregation and toxicity. *ACS Chem. Neurosci. 5*, 148−159.
(58) Cairo, C. W., Strzelec, A., Murphy, R. M., and Kiessling, L. L. (2002) Affinity-based inhibition of beta-amyloid toxicity. *Biochemistry 41*, 8620−8629.
(59) Lande, M. B., Donovan, J. M., and Zeidel, M. L. (1995) The relationship between membrane fluidity and permeabilities to water, solutes, ammonia, and protons. *J. Gen. Physiol. 106*, 67−84.
(60) Walter, A., and Gutknecht, J. (1986) Permeability of small nonelectrolytes through lipid bilayer membranes. *J. Membr. Biol. 90*, 207−217.
(61) McLaurin, J., and Chakrabartty, A. (1997) Characterization of the interactions of Alzheimer beta-amyloid peptides with phospholipid membranes. *Eur. J. Biochem. 245*, 355−363.
(62) Terzi, E., Holzemann, G., and Seelig, J. (1995) Self-association of beta-amyloid peptide(1−40) in solution and binding to lipid-membranes. *J. Mol. Biol. 252*, 633−642.
(63) Chauhan, A., Ray, I., and Chauhan, V. P. S. (2000) Interaction of amyloid beta-protein with anionic phospholipids: Possible involvement of Lys(28) and C-terminus aliphatic amino acids. *Neurochem. Res. 25*, 423−429.
(64) Harper, J. D., Wong, S. S., Lieber, C. M., and Lansbury, P. T. (1999) Assembly of abeta amyloid protofibrils: an in vitro model for a possible early event in Alzheimer's disease. *Biochemistry 38*, 8972−8980.
(65) Ding, T. T., and Harper, J. D. (1999) Analysis of amyloid-beta assemblies using tapping mode atomic force microscopy under ambient conditions, in *Methods in Enzymology* (Wetzel, R., Ed.) pp 510−525, Academic Press, New York.
(66) Tranchida, D., Piccarolo, S., and Deblieck, R. A. C. (2006) Some experimental issues of AFM tip blind estimation: the effect of noise and resolution. *Meas. Sci. Technol. 17*, 2630−2636.
(67) Mattson, M. P. (2004) Pathways towards and away from Alzheimer's disease. *Nature 430*, 631−639.
(68) Etcheberrigaray, R., Hirashima, N., Nee, L., Prince, J., Govoni, S., Racchi, M., Tanzi, R. E., and Alkon, D. L. (1998) Calcium responses in fibroblasts from asymptomatic members of Alzheimer's disease families. *Neurobiol. Dis. 5*, 37−45.
(69) Mattson, M. P., and Chan, S. L. (2003) Calcium orchestrates apoptosis. *Nat. Cell Biol. 5*, 1041−1043.
(70) Larsson, L., and Ohman, S. (1978) Serum ionized calcium and corrected total calcium in borderline hyperparathyroidism. *Clin. Chem. 24*, 1962−1965.
(71) Brini, M., Ottolini, D., Cali, T., and Carafoli, E. (2013) Calcium in health and disease. *Met. Ions Life Sci. 13*, 81−137.
(72) Cherepanov, D. A., Feniouk, B. A., Junge, W., and Mulkidjanian, A. Y. (2003) Low dielectric permittivity of water at the membrane interface: Effect on the energy coupling mechanism in biological membranes. *Biophys. J. 85*, 1307−1316.

DOI: 10.1021/acs.biochem.5b00719
Biochemistry 2015, 54, 6323−6332

(73) Teschke, O., and de Souza, E. F. (2005) Water molecular arrangement at air/water interfaces probed by atomic force microscopy. *Chem. Phys. Lett. 403*, 95−101.
(74) Tofoleanu, F., and Buchete, N.-V. (2012) Alzheimer abeta peptide interactions with lipid membranes fibrils, oligomers and polymorphic amyloid channels. *Prion 6*, 339−345.
(75) Arce, F. T., Jang, H., Ramachandran, S., Landon, P. B., Nussinov, R., and Lal, R. (2011) Polymorphism of amyloid beta peptide in different environments: Implications for membrane insertion and pore formation. *Soft Matter 7*, 5267−5273.
(76) Tsigelny, I. F., Sharikov, Y., Kouznetsova, V. L., Greenberg, J. P., Wrasidlo, W., Gonzalez, T., Desplats, P., Michael, S. E., Trejo-Morales, M., Overk, C. R., and Masliah, E. (2014) Structural diversity of Alzheimer's disease amyloid-beta dimers and their role in oligomerization and fibril formation. *J. Alzheimer's Dis. 39*, 583−600.
(77) Butterfield, S. M., and Lashuel, H. A. (2010) Amyloidogenic protein membrane interactions: Mechanistic insight from model systems. *Angew. Chem., Int. Ed. 49*, 5628−5654.
(78) Homola, J. (2008) Surface plasmon resonance sensors for detection of chemical and biological species. *Chem. Rev. 108*, 462−493.
(79) Sengupta, P., Garai, K., Balaji, J., Periasamy, N., and Maiti, S. (2003) Measuring size distribution in highly heterogeneous systems with fluorescence correlation spectroscopy. *Biophys. J. 84*, 1977−1984.
(80) Cohen, S. I. A., Linse, S., Luheshi, L. M., Hellstrand, E., White, D. A., Rajah, L., Otzen, D. E., Vendruscolo, M., Dobson, C. M., and Knowles, T. P. J. (2013) Proliferation of amyloid-beta 42 aggregates occurs through a secondary nucleation mechanism. *Proc. Natl. Acad. Sci. U. S. A. 110*, 9758−9763.
(81) Subhash, M. N., Padmashree, T. S., Srinivas, K. N., Subbakrishna, D. K., and Shankar, S. K. (1991) Calcium and phosphorus levels in serum and CSF in dementia. *Neurobiol. Aging 12*, 267−269.
(82) Xiong, J., Roach, C. A., Oshokoya, O. O., Schroell, R. P., Yakubu, R. A., Eagleburger, M. K., Cooley, J. W., and Jiji, R. D. (2014) Role of bilayer characteristics on the structural fate of abeta(1−40) and abeta(25−40). *Biochemistry 53*, 3004−3011.
(83) Lockhart, C., and Klimov, D. K. (2014) Alzheimer's Abeta10−40 peptide binds and penetrates DMPC bilayer: an isobaric-isothermal replica exchange molecular dynamics study. *J. Phys. Chem. B 118*, 2638−2648.
(84) Pannuzzo, M., Milardi, D., Raudino, A., Karttunen, M., and La Rosa, C. (2013) Analytical model and multiscale simulations of abeta peptide aggregation in lipid membranes: towards a unifying description of conformational transitions, oligomerization and membrane damage. *Phys. Chem. Chem. Phys. 15*, 8940−8951.

DOI: 10.1021/acs.biochem.5b00719
Biochemistry 2015, 54, 6323−6332